2,2'-Bipyrimidine (bipym)-bridged Dinuclear Complexes. Part 4.[1] Synthesis, Crystal Structure and Magnetic Properties of $[Co_2(H_2O)_8(bipym)][NO_3]_4$, $[Co_2(H_2O)_8(bipym)][SO_4]_2{\cdot}2H_2O$ and $[Co_2(bipym)_3(NCS)_4]$†

Giovanni De Munno,[a] Miguel Julve,*[,b] Francesc Lloret,[b] Juan Faus[b] and Andrea Caneschi[c]

[a] *Dipartimento di Chimica, Università degli Studi della Calabria, 87030 Arcavacata di Rende (Cosenza), Italy*

[b] *Departament de Química Inorgànica, Facultat de Química de la Universitat de València, Dr. Moliner 50, 46100 Burjassot (València), Spain*

[c] *Dipartimento di Chimica, Università degli Studi di Firenze, Via Maragliano 75/77, 50144 Firenze, Italy*

Three new dinuclear cobalt(II) complexes $[Co_2(H_2O)_8(bipym)][NO_3]_4$ **1**, $[Co_2(H_2O)_8(bipym)][SO_4]_2{\cdot}2H_2O$ **2** and $[Co_2(bipym)_3(NCS)_4]$ **3** (bipym = 2,2'-bipyrimidine) have been synthesised and their crystal structures determined by X-ray diffraction methods. Crystals of **1** and **3** are triclinic, space group $P\bar{1}$, $Z = 1$ with $a = 7.511(1)$, $b = 8.844(2)$, $c = 9.514(1)$ Å, $\alpha = 79.67(1)$, $\beta = 88.54(1)$ and $\gamma = 82.46(1)°$ for **1** and $a = 9.045(2)$, $b = 9.149(2)$, $c = 11.621(2)$ Å, $\alpha = 74.73(2)$, $\beta = 80.67(2)$ and $\gamma = 61.17(1)°$ for **3**. Crystals of **2** are monoclinic, space group $P2_1/c$ with $a = 8.115(1)$, $b = 11.596(2)$, $c = 11.823(3)$ Å, $\beta = 91.57(2)°$ and $Z = 2$. The structures of **1** and **2** are made up of dinuclear cations $[Co_2(H_2O)_8(bipym)]^{4+}$ with nitrate counter ions for **1** and water of crystallization and sulfate groups for **2**. The structure of **3** consists of dimeric neutral $[Co_2(bipym)_3(NCS)_4]$ units. Bipyrimidine bridges the cobalt atoms in this series of complexes in a bis(chelating) fashion and a crystallographically imposed inversion centre is located halfway between its two pyrimidyl rings. It is present also as a terminal ligand in **3**. The two equivalent cobalt atoms of **1** and **2** are each bound to four water oxygens and two *cis* nitrogens of bipym in a slightly distorted octahedral environment. Each cobalt atom in **3** is bound to six nitrogen atoms belonging to two thiocyanate groups in *cis* position and to two bipym ligands, one terminal and the other bridging. The intramolecular metal–metal separation varies between 5.761(1) and 5.942(2) Å. The magnetic properties of **1**–**3** have been investigated in the temperature range 4.2–300 K. They all exhibit antiferromagnetic exchange with susceptibility maxima at 13.0–16.4 K. Fits of the magnetic data through the Lines model and the simpler Ising spin-only formalism are compared.

During the last decade several reports concerning the structure and magnetic properties of 2,2'-bipyrimidine (bipym)-containing copper(II) complexes have been published.[2–9] These investigations have illustrated both the versatility of bipym as a ligand and its noticeable ability to transmit magnetic interactions between copper(II) ions separated by distances larger than 5.5 Å. Values of J (singlet–triplet energy gap) up to -236 cm^{-1} were achieved when the σ in-plane exchange pathway is operative (large σ in-plane overlap of the two d_{xy} magnetic metal orbitals through the bipym bridge).[2b]

The bridging ability of bipym towards other first-row transition-metal ions such as cobalt(II),[10] nickel(II),[11] iron(II)[12,13] and zinc(II)[1] has been explored and the study of the magnetic properties of structurally characterized dinuclear $[M^{II}_2(bipym)]^{4+}$ complexes (M = Fe, Co or Ni) revealed the occurrence of relatively weak intradimer antiferromagnetic interactions. As far as cobalt is concerned, the magnetic study of dinuclear complexes $[L_2Co(bipym)CoL_2]$ [L = hexafluoroacetylacetonate (hfacac), trifluoroacetylacetonate (tfacac) or trifluoro(phenyl)acetyl acetonate (ptfacac)] revealed that the extent of coupling is practically independent of the complexity of L.[10] The susceptibilities were analysed in terms of the spin-only formula for homodinuclear complexes with an isotropic exchange interaction, in spite of the large orbital contribution to the magnetic moment which would be involved according to the slightly distorted octahedral environment of the metal ion in this series.

As an extension of our current research work concerning bipym-bridged homodinuclear complexes, we report here the preparation and structural and magnetic characterization of three bipym-containing cobalt(II) complexes, $[Co_2(H_2O)_8(bipym)][NO_3]_4$ **1**, $[Co_2(H_2O)_8(bipym)][SO_4]_2{\cdot}2H_2O$ **2** and $[Co_2(bipym)_3(NCS)_4]$ **3**. The influence of spin–orbit coupling on the value of J in this series is analysed and discussed.

Experimental

Materials.—2,2'-Bipyrimidine was obtained from Lancaster Synthesis and used without further purification. The compounds $Co(NO_3)_2{\cdot}6H_2O$, $CoSO_4{\cdot}7H_2O$ and $Co(NCS)_2$ were obtained from Strem Chemicals and used as received. Elemental analyses (C, H, N) were by the Microanalytical Service of the University of Cosenza (Italy). The metal content was determined by atomic absorption spectrometry.

Preparations.—$[Co_2(H_2O)_8(bipym)][NO_3]_4$ **1**. This compound was prepared by mixing aqueous solutions of bipym (0.5 mmol, 5 cm^3) and cobalt(II) nitrate hexahydrate (1 mmol, 15 cm^3). Chunky peach-pink crystals of complex **1** separated when nearly all the solvent was evaporated at room temperature. Crystals suitable for X-ray analysis were obtained by cutting

† *Supplementary data available:* see Instructions for Authors, *J. Chem. Soc., Dalton Trans.*, 1994, Issue 1, pp. xxiii–xxviii.

Non-SI units employed: emu = SI × $10^6/4\pi$, $\mu_B \approx 9.27 \times 10^{-24}$ J T^{-1}.

some of these. The remaining product was collected and washed with small amounts of a cooled ethanol–water mixture and stored over calcium chloride. The occurrence of a very asymmetric doublet at 1585s and 1565w cm^{-1} (ring-stretching modes of bipym) in the IR spectrum of **1** and at practically the same wavenumbers for **2** is common to a series of compounds containing bis(chelating) bipym which have been structurally characterized.[5a,8,9,11,13] This suggests that bipym acts as a bridging ligand in **1** and **2** in full agreement with their crystal structures (Found: C, 14.25; H, 3.15; Co, 17.10; N, 16.80. Calc. for $C_8H_{22}Co_2N_8O_{20}$: C, 14.40; H, 3.30; Co, 17.65; N, 16.75%).

$[Co_2(H_2O)_8(bipym)][SO_4]_2 \cdot 2H_2O$ **2**. This complex was obtained in two crystalline forms, pink plates and amber prisms, by slow evaporation at room temperature of aqueous solutions (30 cm^3) containing bipym (0.5 mmol) and cobalt(II) sulfate heptahydrate (1 mmol). Only the prismatic crystals were suitable for X-ray diffraction. Recrystallization of the plates in water yielded nice crystals of the other crystalline form. Identical analytical results (C, H, N, Co) were obtained for both types of crystals, supporting the same formulation (Found: C, 14.50; H, 3.95; Co, 17.85; N, 8.45. Calc. for $C_8H_{26}Co_2N_4O_{18}S_2$: C, 14.85; H, 4.00; Co, 18.20; N, 8.65%).

$[Co_2(bipym)_3(NCS)_4]$ **3**. This compound was obtained as an orange-red powder by adding an ethanolic solution of bipym (0.3 mmol, 10 cm^3) to an aqueous solution of cobalt(II) thiocyanate (0.2 mmol, 10 cm^3). It was filtered off, washed with water and ethanol and stored over calcium chloride. Polyhedral single crystals of **3** were grown by slow evaporation of aqueous solutions (150 cm^3) containing bipym (1 mmol) and cobalt(II) thiocyanate (0.5 mmol). The presence of two sharp absorptions at 1570s and 1550m cm^{-1} in the IR spectrum, which has been observed for structurally characterized compounds containing chelating bipym,[4,5a,8] supports the occurrence of terminal bipym in **3**. The appearance of an intense doublet at 2090 and 2070 and a single sharp band at 475 cm^{-1}, assigned to C–N and Co–N (thiocyanate) stretching vibrations,[14,15] are indicative of thiocyanato-*N* bonding. These spectroscopic assignments have been confirmed by X-ray diffraction (Found: C, 40.55; H, 2.15; Co, 13.95; N, 27.00. Calc. for $C_{28}H_{18}Co_2N_{16}S_4$: C, 40.80; H, 2.20; Co, 14.30; N, 27.15%).

Physical Techniques.—The infrared spectra were recorded on a Perkin Elmer 1750 FTIR spectrophotometer as KBr pellets in the 4000–300 cm^{-1} region. Variable-temperature magnetic susceptibility measurements were carried out in the range 4.2–300 K with a fully automatized AZTEC DSM8 pendulum-type susceptometer equipped with a TBT continuous-flow cryostat and a Brüker BE15 electromagnet, operating at 1.8 T. The apparatus was calibrated with $Hg[Co(NCS)_4]$. Corrections for the diamagnetism of complexes **1–3** were estimated from Pascal's constants[16] as -304×10^{-6}, -334×10^{-6} and -448×10^{-6} emu mol^{-1}, respectively.

Crystal Structure Determination and Refinement.—Diffraction data for complexes **1–3** were collected at room temperature with a Siemens R3m/V automatic four-circle diffractometer using graphite-monochromated Mo-Kα radiation (λ = 0.710 73 Å). Information concerning crystallographic data collection and refinement of the structures is summarized in Table 1. The unit-cell parameters were determined from least-squares refinement of the setting angles of 25 reflections in the range 2θ 15–30°. The intensity data were collected in the index ranges $0 \leqslant h \leqslant 9$, $-11 \leqslant k \leqslant 11$, $-12 \leqslant l \leqslant 12$ for **1**, $0 \leqslant h \leqslant 10$, $0 \leqslant k \leqslant 14$, $-15 \leqslant l \leqslant 15$ for **2** and $0 \leqslant h \leqslant 11$, $-10 \leqslant k \leqslant 10$, $-14 \leqslant l \leqslant 14$ for **3**. Examination of three standard reflections, monitored after every 100, showed no sign of crystal deterioration. Lorentz-polarization and ψ-scan absorption corrections[17] were applied to the intensity data. The space group $P\bar{1}$ was assumed for **1** and **3** and this choice was later confirmed by the successful refinement of their structures. The data collection for **2** showed systematic absences ($h0l$, $l = 2n + 1$; $0k0$, $k = 2n + 1$) consistent with the monoclinic space group $P2_1/c$ (no. 14). The maximum and minimum transmission factors were 0.607 and 0.760 for **1**, 0.427 and 0.462 for **2** and 0.822 and 0.944 for **3**.

The structures of complexes **1–3** were solved by standard Patterson methods with the SHELXTL PLUS program[18] and subsequently completed by Fourier recycling. All non-hydrogen atoms were refined anisotropically. The hydrogen atoms of the water molecules were located on a ΔF map and refined with constraints. The hydrogen atoms of bipym were set in calculated positions and refined as riding atoms. A common fixed isotropic

Table 1 Crystallographic data[a] for complexes **1–3**

	1	**2**	**3**
Formula	$C_8H_{22}Co_2N_8O_{20}$	$C_8H_{26}Co_2N_4O_{18}S_2$	$C_{28}H_{18}Co_2N_{16}S_4$
M	668.2	648.3	824.7
Crystal system	Triclinic	Monoclinic	Triclinic
Space group	$P\bar{1}$	$P2_1/c$	$P\bar{1}$
a/Å	7.511(1)	8.115(1)	9.045(2)
b/Å	8.844(2)	11.596(2)	9.149(2)
c/Å	9.514(1)	11.823(3)	11.621(2)
α/°	79.67(1)	90	74.73(2)
β/°	88.54(1)	91.57(2)	80.67(2)
γ/°	82.46(1)	90	61.17(1)
U/Å^3	616.4(2)	1112.1(4)	812.0(3)
Z	1	2	1
D_c/kg m^{-3}	1.800	1.936	1.686
F(000)	340	664	416
Crystal size/mm	0.18 × 0.16 × 0.42	0.23 × 0.31 × 0.42	0.10 × 0.18 × 0.32
μ(Mo-Kα)/cm^{-1}	14.4	17.6	13.2
2θ range/°	3–55	3–54	3–54
No of reflections collected	3062	2810	3805
No. of unique reflections	2844	2442	3574
No. of independent reflections,[b] N_o	2470	2191	2782
No. of refined parameters, N_p	196	184	226
R[c]	0.0290	0.0260	0.0275
R'[d]	0.0325	0.0306	0.0282
S[e]	1.17	1.21	1.34

[a] Details in common: T = 298 K, ω–2θ scan method. [b] $I > 3\sigma(I)$. [c] $R = [\Sigma(||F_o| - |F_c||)\Sigma|F_o|]$. [d] $R' = [\Sigma(||F_o| - |F_c||)^2/\Sigma w|F_o|^2]^{\frac{1}{2}}$. [e] Goodness of fit $= [\Sigma w(||F_o| - |F_c||)^2/(N_o - N_p)]^{\frac{1}{2}}$.

thermal parameter was assigned to all hydrogen atoms. The final full-matrix least-squares refinement, minimizing the function $\Sigma w(||F_o| - |F_c||)^2$ with $w = 1/[\sigma^2(F_o) + q(F_o)^2]$ (q = 0.001 000 for **1**, 0.001 000 for **2** and 0.000 181 for **3**) [with $\sigma^2(F_o)$ from counting statistics], converged at R and R' indices of 0.0290 and 0.0325, 0.0260 and 0.0306 and 0.0275 and 0.0282 respectively. The number of reflections/number of variable parameters was 12.6, 11.9 and 12.3, respectively. In the final difference map the residual maxima and minima were 0.30 and −0.56, 0.37 and −0.60 and 0.24 and −0.29 e Å^{-3}. The largest and mean Δ/σ are 0.023 and 0.002, 0.573 and 0.044 and 0.009 and 0.003. Solutions and refinements were performed with the SHELXTL PLUS system,[18] final geometrical calculations with the PARST[19] program and graphical manipulations using the XP utility of the SHELXTL PLUS system. The final atomic coordinates for non-hydrogen atoms and selected bond lengths and angles are given in Tables 2–7.

Additional material available from the Cambridge Crystallographic Data Centre comprises H-atom coordinates, thermal parameters, and remaining bond lengths and angles.

Results and Discussion

The Structures of Complexes **1** *and* **2**.—The structures of complexes **1** and **2** are made up of μ-(2,2′-bipyrimidine-*N*,*N*′,*N*″,*N*‴)-bis[tetraaquacobalt(II)] dinuclear cations with a crystallographically imposed inversion centre located halfway between the halves of the bipym molecule, and unco-ordinated nitrate (**1**) and sulfate (**2**) anions. Two water molecules of crystallization are also present in **2**. The molecular geometry and the atom labelling scheme for the cation of **1** (identical labelling was used for **2**) is illustrated in Fig. 1. The counter ions contribute to the packing by forming an extensive network of hydrogen bonds involving both co-ordinated and unco-

Table 2 Final atomic coordinates for compound **1** with estimated standard deviations (e.s.d.s) in parentheses

Atom	*X*/*a*	*Y*/*b*	*Z*/*c*
Co(1)	0.0608(1)	0.1977(1)	0.2325(1)
O(1)	0.2376(2)	0.1698(2)	0.0660(2)
O(2)	−0.0759(2)	0.4056(2)	0.1367(2)
O(3)	−0.1104(2)	0.0881(2)	0.1255(2)
O(4)	0.2400(2)	0.3159(2)	0.3203(2)
N(1)	0.1710(2)	−0.0155(2)	0.3668(2)
C(1)	0.3193(3)	−0.1113(3)	0.3464(2)
C(2)	0.3744(3)	−0.2417(3)	0.4456(3)
C(3)	0.2712(3)	−0.2721(2)	0.5664(2)
N(2)	0.1203(2)	−0.1785(2)	0.5868(2)
C(4)	0.0810(2)	−0.0536(2)	0.4872(2)
N(3)	0.5783(2)	0.3670(2)	0.9056(2)
O(5)	0.7056(2)	0.4446(2)	0.9000(2)
O(6)	0.4604(2)	0.3977(2)	0.8150(2)
O(7)	0.5733(2)	0.2566(3)	1.0077(3)
N(4)	0.1519(3)	0.2795(2)	0.6861(2)
O(8)	0.0746(2)	0.2953(2)	0.8009(2)
O(9)	0.2240(3)	0.1488(2)	0.6690(2)
O(10)	0.1590(3)	0.3935(2)	0.5904(2)

Table 3 Final atomic coordinates for compound **2** with (e.s.d.s) in parentheses

Atom	*X*/*a*	*Y*/*b*	*Z*/*c*
Co(1)	0.1842(1)	0.1057(1)	0.1853(1)
S(1)	0.7285(1)	0.2837(1)	−0.0196(1)
O(1)	0.4214(2)	0.1766(1)	0.2128(1)
O(2)	0.1191(2)	0.1409(2)	0.3503(1)
O(3)	0.1081(2)	0.2712(1)	0.1437(1)
O(4)	0.2701(2)	−0.0568(1)	0.2381(1)
O(5)	0.8406(2)	0.2295(1)	−0.1000(1)
O(6)	0.6047(2)	0.3547(2)	−0.0821(1)
O(7)	0.8264(2)	0.3618(1)	0.0550(1)
O(8)	0.6473(2)	0.1956(2)	0.0469(1)
O(9)	0.3241(2)	0.4084(1)	0.0332(2)
N(1)	0.2033(2)	0.0613(1)	0.0073(1)
C(1)	0.3275(3)	0.0801(2)	−0.0635(2)
C(2)	0.3177(2)	0.0463(2)	−0.1759(2)
C(3)	0.1772(2)	−0.0095(2)	−0.2123(2)
N(2)	0.0514(2)	−0.0291(1)	−0.1432(1)
C(4)	0.0702(2)	0.0089(2)	−0.0373(1)

Table 4 Final atomic coordinates for compound **3** (e.s.d.s) in parentheses

Atom	*X*/*a*	*Y*/*b*	*Z*/*c*
Co(1)	0.2066(1)	0.2404(1)	0.2016(1)
N(5)	0.2571(3)	0.2698(3)	0.3558(2)
C(5)	0.2946(3)	0.2755(3)	0.4444(2)
S(1)	0.3507(1)	0.2800(1)	0.5689(1)
N(6)	0.4210(3)	0.2467(3)	0.1150(2)
C(6)	0.5437(3)	0.2609(3)	0.0985(2)
S(2)	0.7175(1)	0.2782(1)	0.0737(1)
N(1)	0.0371(2)	0.5127(2)	0.1436(1)
C(1)	−0.0054(3)	0.6337(3)	0.2050(2)
C(2)	−0.0987(3)	0.8039(3)	0.1552(2)
C(3)	−0.1484(3)	0.8464(2)	−0.0220(2)
N(2)	−0.1116(2)	0.7277(2)	−0.0220(2)
C(4)	−0.0208(2)	0.5669(3)	0.0334(2)
N(3)	0.0070(2)	0.1893(2)	0.3010(2)
C(7)	−0.1348(3)	0.2985(3)	0.3496(2)
C(8)	−0.2535(3)	0.2510(3)	0.4101(2)
C(9)	−0.2207(3)	0.0857(3)	0.4187(2)
N(7)	−0.0771(3)	−0.0292(3)	0.3758(2)
C(10)	0.0301(3)	0.0297(3)	0.3196(2)
C(11)	0.1956(3)	−0.0930(3)	0.2735(2)
N(8)	0.2279(3)	−0.2546(2)	0.2873(2)
C(12)	0.3784(3)	−0.3577(3)	0.2430(2)
C(13)	0.4946(3)	−0.3031(3)	0.1895(2)
C(14)	0.4512(3)	−0.1353(3)	0.1803(2)
N(4)	0.3007(2)	−0.0273(2)	0.2224(2)

Table 5 Selected interatomic distances (Å) and angles (°) for compound **1** with e.s.d.s in parentheses *

Co(1)–O(1)	2.069(2)	Co(1)–O(4)	2.083(2)
Co(1)–O(2)	2.053(1)	Co(1)–N(1)	2.157(2)
Co(1)–O(3)	2.093(2)	Co(1)–N(2a)	2.161(2)
O(1)–Co(1)–O(2)	96.6(1)	O(2)–Co(1)–O(4)	89.8(1)
O(1)–Co(1)–N(2a)	168.9(1)	O(3)–Co(1)–N(2a)	89.0(1)
O(1)–Co(1)–N(1)	94.2(1)	O(3)–Co(1)–N(1)	93.4(1)
O(1)–Co(1)–O(3)	85.3(1)	O(3)–Co(1)–O(4)	174.6(1)
O(1)–Co(1)–O(4)	90.2(1)	N(1)–Co(1)–N(2a)	76.6(1)
O(2)–Co(1)–N(2a)	92.7(1)	N(1)–Co(1)–O(4)	89.9(1)
O(2)–Co(1)–N(1)	169.2(1)	N(2a)–Co(1)–O(4)	95.9(1)
O(2)–Co(1)–O(3)	87.8(1)		

* Symmetry code: a $-x, -y, 1-z$.

Table 6 Selected interatomic distances (Å) and angles (°) for compound **2** with e.s.d.s in parentheses *

Co(1)–O(1)	2.110(2)	Co(1)–O(4)	2.098(2)
Co(1)–O(2)	2.075(2)	Co(1)–N(1)	2.177(2)
Co(1)–O(3)	2.072(2)	Co(1)–N(2a)	2.154(2)
O(1)–Co(1)–O(2)	91.9(1)	O(2)–Co(1)–O(4)	89.3(1)
O(1)–Co(1)–N(2a)	175.1(1)	O(3)–Co(1)–N(2a)	94.0(1)
O(1)–Co(1)–N(1)	98.8(1)	O(3)–Co(1)–N(1)	91.1(1)
O(1)–Co(1)–O(3)	86.6(1)	O(3)–Co(1)–O(4)	175.8(1)
O(1)–Co(1)–O(4)	90.6(1)	N(1)–Co(1)–N(2a)	76.4(1)
O(2)–Co(1)–N(2a)	92.9(1)	N(1)–Co(1)–O(4)	92.5(1)
O(2)–Co(1)–N(1)	169.2(1)	N(2a)–Co(1)–O(4)	89.1(1)
O(2)–Co(1)–O(3)	87.6(1)		

* Symmetry code: a $-x, -y, -z$.

Table 7 Selected interatomic distances (Å) and angles (°) for compound **3** with e.s.d.s in parentheses *

Cobalt environment			
Co(1)–N(1)	2.185(2)	Co(1)–N(4)	2.127(2)
Co(1)–N(2a)	2.279(2)	Co(1)–N(5)	2.032(3)
Co(1)–N(3)	2.161(2)	Co(1)–N(6)	2.055(2)
N(1)–Co(1)–N(2a)	73.7(1)	N(2a)–Co(1)–N(6)	89.1(1)
N(1)–Co(1)–N(4)	157.5(1)	N(3)–Co(1)–N(4)	75.6(1)
N(1)–Co(1)–N(5)	93.3(1)	N(3)–Co(1)–N(5)	87.3(1)
N(1)–Co(1)–N(3)	93.0(1)	N(3)–Co(1)–N(6)	170.6(1)
N(1)–Co(1)–N(6)	96.4(1)	N(4)–Co(1)–N(5)	105.3(1)
N(2a)–Co(1)–N(4)	87.3(1)	N(4)–Co(1)–N(6)	95.4(1)
N(2a)–Co(1)–N(5)	167.1(1)	N(5)–Co(1)–N(6)	92.7(1)
N(2a)–Co(1)–N(3)	93.1(1)		
Thiocyanate ligand			
N(5)–C(5)	1.157(4)	N(6)–C(6)	1.159(4)
C(5)–S(1)	1.626(3)	C(6)–S(2)	1.627(3)
Co(1)–N(5)–C(5)	175.4(2)	Co(1)–N(6)–C(6)	159.2(2)
N(5)–C(5)–S(1)	178.9(2)	N(6)–C(6)–S(2)	178.8(2)

* Symmetry code: a $-x, 1-y, -z$.

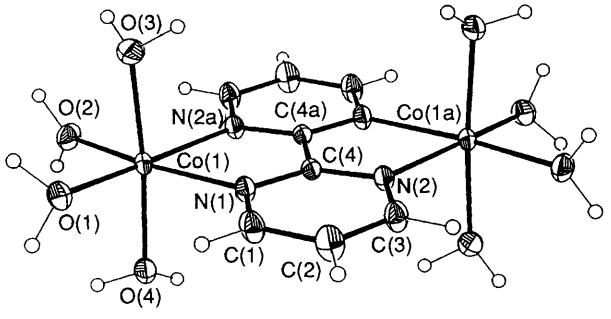

Fig. 1 A perspective view of the cationic unit $[Co_2(H_2O)_8(bipym)]^{4+}$ of **1** showing the atom labelling. Thermal ellipsoids are drawn at the 30% probability level

ordinated water molecules. Complex **2** is isostructural with the $[M_2(H_2O)_8(bipym)][SO_4]_2{\cdot}2H_2O$ (M = Ni^{II}, Fe^{II} and Zn^{II})[1,11,13] complexes.

Each cobalt atom in complexes **1** and **2** is six-co-ordinated in a slightly distorted octahedral CoN_2O_4 chromophore: two nitrogen atoms from bipym in *cis* position and four oxygen atoms from water molecules comprise the co-ordination polyhedra. The bipym group acts as a bis(chelating) ligand and joins two adjacent octahedra, the carbon–carbon bond between the pyrimidine rings being perpendicular to the Co···Co vector in the dimeric unit. The average cobalt to nitrogen bond distance is larger [2.159(2) in **1** and 2.166(2) Å in **2**] than that of cobalt to oxygen [2.075(2) in **1** and 2.089(2) Å in **2**]. The Co–N (bipym) bond lengths in **1** and **2** are practically identical to that found in the compound $[(hfacac)_2Co(bipym)Co(hfacac)_2]$,[10] whereas the Co–O(water) distances are somewhat larger than those of Co–O(hfacac) [average 2.051(3) Å]. The best equatorial plane is defined by the N(1), N(2a), O(1) and O(2) atoms [largest deviations 0.068(2) Å for N(2a) in **1** and 0.028(3) Å for O(2) in **2**]. The cobalt atom is 0.048(1) (**1**) and 0.012(1) Å (**2**) out of this plane. Significant deviations from idealized orthogonal geometry are found at the cobalt atom in the five-membered Co(1)N(1)C(4)C(4a)N(2a) chelate ring [76.6(1) and 76.4(1)° for N(1)–Co(1)–N(2a) in **1** and **2**, respectively] which are due to the short bite distance of the unco-ordinated bipym (2.63 Å).[20] The value of the angle subtended at the metal atom by bipym in the complexes $[(H_2O)_4M(bipym)M(H_2O)_4]^{4+}$ follows the trend Ni > Co > Zn > Fe in full agreement with the lengthening of the N–N(bipym) bond distance along this series.

The pyrimidyl rings of bipym are planar [largest deviations from the mean N(1)C(1)C(2)C(3)N(2)C(4) plane 0.013(2) and 0.012(2) Å for C(4) in **1** and **2**, respectively] as is the ligand as a whole. The carbon–carbon and –nitrogen intra-ring bonds are very similar to those observed in both unco-ordinated and co-ordinated bipym. The carbon–carbon inter-ring bond lengths [1.485(3) and 1.474(4) Å in **1** and **2**, respectively] are somewhat reduced with respect to the expected value for a single carbon–carbon bond distance. The cobalt atom is 0.006(1) (**1**) and 0.050(1) Å (**2**) out of the bipym plane. The dihedral angle between the bipym and the equatorial N(1)N(2a)O(1)O(2) planes is 4.1(1)° for **1** and 2.3(1)° for **2**. The metal–metal separation through bipym, Co(1)···Co(1a), is 5.761(1) Å in **1** and 5.782(1) Å in **2**, whereas the shortest intermolecular metal–metal separation is somewhat larger [6.264(1) Å for Co(1)···Co(1g) (g at $-x, -y, -z$) in **1** and 6.719(1) Å for Co(1)···Co(1h) and Co(1)···Co(1i) (h at $-x, y-\frac{1}{2}, -z+\frac{1}{2}$; i at $-x, y+\frac{1}{2}, -z+\frac{1}{2}$) in **2**].

The nitrate and sulfate anions have their expected trigonal and tetrahedral geometries, respectively. The nitrogen–oxygen bond lengths and the intra-anion bond angles average 1.241(3) Å and 120.0(2)°, respectively. The average sulfur–oxygen bond distance and intra-ion bond angle for the sulfate group are 1.473(2) Å and 109.5(1)°.

The Structure of Complex **3**.—The structure of complex **3** consists of centrosymmetric discrete dinuclear molecules, in which the two cobalt(II) ions are bridged by a bipym ligand in a bis(chelating) fashion. A structural representation with the atom labelling is shown in Fig. 2.

Each cobalt atom is bound to six nitrogen atoms belonging to two thiocyanate groups in *cis* position and two bipym ligands, one terminal and the other bridging. The Co–N bond lengths involving thiocyanate [2.032(3) and 2.055(2) Å for Co(1)–N(5) and Co(1)–N(6)] are much shorter than those involving the bridging [2.185(2) and 2.279(2) Å for Co(1)–N(1) and Co(1)–N(2a)] and terminal [2.161(2) and 2.127(2) Å for Co(1)–N(3) and Co(1)–N(4)] bipym ligands. The geometry of complex **3** is very similar to that of $[Fe_2(bipym)_3(NCS)_4]$[12] except for the presence of iron instead of cobalt. Also in this latter compound the two Fe–N bonds involving the bridging bipym are significantly different [2.316(6) and 2.223(6) Å]. No relevant differences in the bond distances of the organic ligand were found. The best equatorial plane is defined by atoms N(1), N(2a), N(5) and N(4) [maximum deviation 0.120(3) Å for N(5)]. The cobalt atom is 0.141(1) Å out of this plane. The bite angles of the terminal [75.6(1)° for N(3)–Co(1)–N(4)] and bridging [73.7(1)° for N(1)–Co(1)–N(2a)] bipym ligands are somewhat different as a consequence of the different Co–N (bipym) bond lengths.

All pyrimidyl rings are planar as expected with deviations from the mean planes not greater than 0.013(3) and 0.024(3) Å for bridging and terminal bipym groups, respectively. The two pyrimidine rings from the terminal bipym form a dihedral angle of 3.6(1)°, while they are coplanar in the central bipym. The inter-ring carbon–carbon bond length for bridging [1.484(5) Å for C(4)–C(4a)] and terminal [1.492(3) Å] bipym groups are practically identical. Whereas the N–C–S groups are quasi-linear a significant bending is displayed by the Co–N–C(S) linkages [175.4(2) and 159.2(2)° for Co(1)–N(5)–C(5) and Co(1)–N(6)–C(6), respectively].

The arrangement of the molecules in complex **3** shows graphitic interactions between the terminal bipym ligands [3.405(4) Å for C(9)···C(10b); symmetry code b at $-x, -y, 1-z$] from adjacent dinuclear units leading to linear chains which are interconnected by van der Waals interactions. This arrangement is very similar to that found in the compound $[Cu_2(H_2O)_4(bipym)_3][ClO_4]_4$,[6a] the distance between the facing rings being 3.336(4) Å in this compound and 3.378(3) Å in **3**. The intramolecular metal–metal separation, Co(1)···Co(1a), is 5.942(2) Å, a value significantly longer than that in **1**

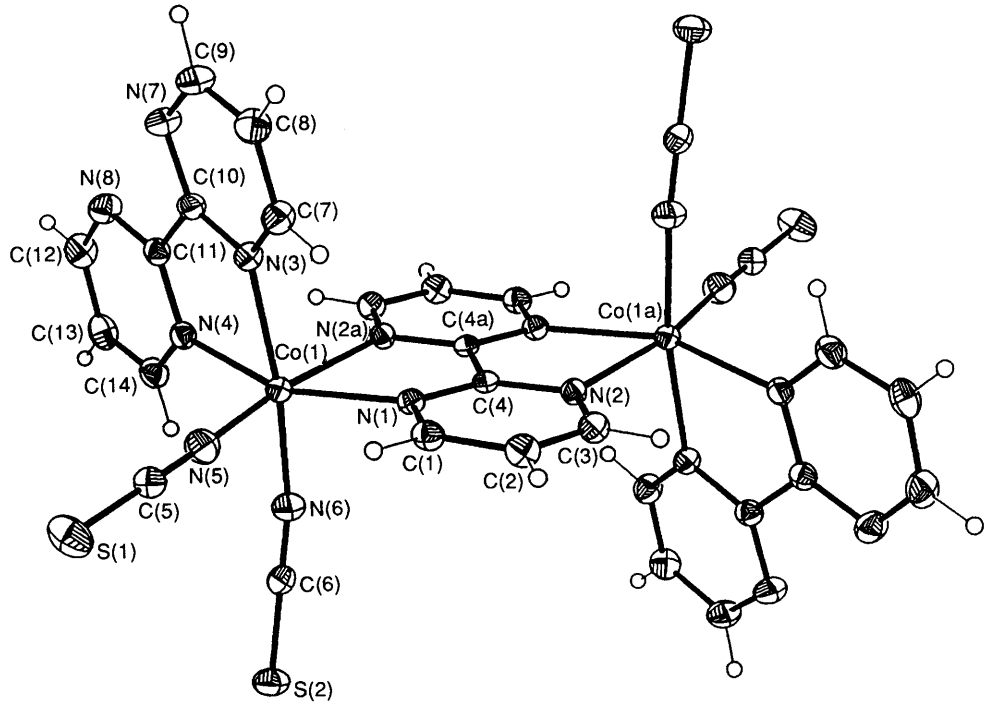

Fig. 2 A perspective view of complex **3** showing the atom labelling; thermal ellipsoids are drawn at the 30% probability level

and **2** due to the lengthening of the Co–N (bridging bipym) bonds in **3**. The shortest intermolecular metal–metal separation Co(1) · · · Co(1c) (symmetry code c at $-x, -y, -z$) is 7.054(2) Å.

Magnetic Properties.—The magnetic properties of complexes **1**–**3** in the form of plots of both χ_M (molar magnetic susceptibility) and $\chi_M T$ *versus* T are depicted in Fig. 3. The susceptibility curves show rounded maxima at 13.5 (**1**), 13.0 (**2**) and 16.4 K (**3**), whereas those of $\chi_M T$ exhibit a continuous decrease upon cooling, with $\chi_M T = 6.35$ (μ_{eff} per $Co^{II} = 5.04$) (**1**), 6.32 (5.03) (**2**) and 5.35 cm^3 K mol^{-1} (4.63 μ_B) (**3**) at 290 K and an extrapolated value which vanishes when T approaches zero. The values of μ_{eff} per cobalt atom at room temperature are larger than that expected for the spin-only case ($\mu_{eff} = 3.87$ μ_B, $S = \frac{3}{2}$) indicating that an important orbital contribution is involved. The occurrence of maxima in χ_M is indicative of the existence of antiferromagnetic coupling between the paramagnetic centres.

In order to evaluate the exchange coupling (J) for this family of dinuclear cobalt(II) complexes, we first analysed the experimental magnetic data through the simple expression (1)

$$\hat{H} = -J\hat{S}_A \cdot \hat{S}_B \quad (1)$$

implying an isotropic Heisenberg form of interaction with $S_A = S_B = \frac{3}{2}$. This was unsuccessful because the distortion of the octahedral symmetry of Co^{II} in **1**–**3** is not so large as to induce total quenching of the orbital moment of the $^4T_{1g}$ ground state. When the single-ion ground state is orbitally degenerate the orbital effects cannot be considered merely as a perturbation in the isotropic exchange and there are no limits on their magnitude relative to the isotropic exchange.[21] The general Hamiltonian operators derived to treat this problem involve such a large number of parameters as to make them practically useless in interpreting the magnetic susceptibility data for polynuclear systems.[22] Drastic approximations must be introduced in the Hamiltonians in order to obtain significant information about the exchange coupling in these compounds. The Lines' theory[23] of polynuclear compounds of Co^{II} is the only one that has been presented in this regard.

For octahedral high-spin Co^{II} the single-ion excited states are well separated (> 8000 cm^{-1}) from the ground state and can be neglected. The $^4T_1$ ground state is split into a sextet, a quartet and a Kramer's doublet by spin–orbit coupling. The eigenvalues and eigenfunctions are found by diagonalizing the operator (2)

$$-\tfrac{3}{2}x\lambda\hat{L}\cdot\hat{S} \quad (2)$$

within the $|m_l,m_s>$ representation, where $m_l = 0, \pm 1$ and $m_s = \pm\frac{1}{2}, \pm\frac{3}{2}$ (x and λ being the orbital reduction factor and the spin–orbit coupling parameters, respectively). The occurrence of the factor $-\frac{3}{2}$ is due to the analogy between the matrix elements of L within the $^4T_1$ state and that of $-\frac{3}{2}L$ between the p functions $|1, 1>$, $|1, 0>$ and $|1, -1>$. The values of the energies of the doublet, quartet and sextet levels are $\frac{15}{4}x\lambda$, $\frac{3}{2}x\lambda$ and $-\frac{9}{4}x\lambda$, respectively. Restricting ourselves to the ground Kramers doublet, it has been shown that expression (3) applies

$$\hat{S} = \tfrac{3}{5}\hat{s} \quad (3)$$

where s is an effective spin $\frac{1}{2}$. The resulting effective spin $\frac{1}{2}$ Hamiltonian for the dimer, assuming the coupling between cobalt(II) ions is isotropic, is given by equation (4) where

$$\hat{H} = \tfrac{25}{9}J\hat{s}_A\cdot\hat{s}_B + g_0\beta H_z(\hat{s}_{A,z} + \hat{s}_{B,z}) \quad (4)$$

$g_0 = (\frac{10}{3} + x)$ and H_z is the magnetic field in the z direction. This Hamiltonian can easily be diagonalized and the corresponding expression for the molar susceptibility is (5) where

$$\chi_M = (2N\beta^2 g_0^2/kT)[3 + \exp(-25J/9kT)]^{-1} \quad (5)$$

N, β and k have their usual meanings. When the large anisotropy which is characteristic of Co^{II} ($g_{\|} \neq g_{\perp}$) is introduced, the resulting expression for χ_M involving two spin doublets (Ising dimer) is (6).[24] Equations (5) and (6)–(8) can

$$\chi_M = (\chi_{\|} + 2\chi_{\perp})/3 \quad (6)$$

$$\chi_{\|} = (N\beta^2 g_{\|}^2/2kT)[\exp(25J/18kT)]/\cosh(25J/18kT) \quad (7)$$

$$\chi_{\perp} = (18N\beta^2 g_{\perp}^2/25J)\tanh(25J/36kT) \quad (8)$$

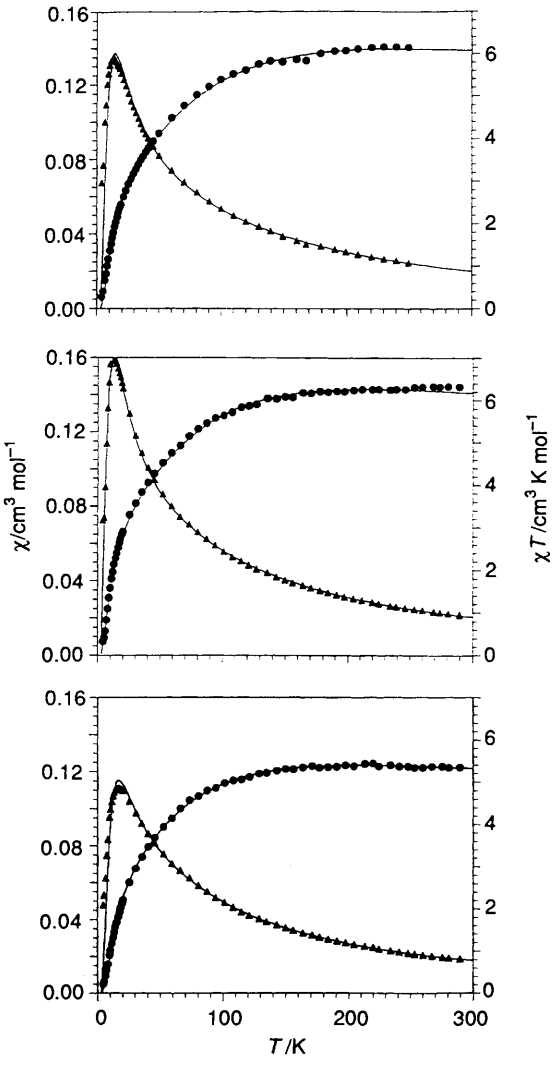

Fig. 3 Thermal dependence of the molar magnetic susceptibility χ_M (▲) and $\chi_M T$ (●) for complexes **1** (top), **2** (middle) and **3** (bottom). The solid lines correspond to the best theoretical fits (see text)

be used to analyse the susceptibility data at $T < 30$ K, that is in the temperature range where it is possible to assume that only the Kramer's doublet for Co^{II} remains populated. Given that the energy separation between the quartet and ground-state doublet is *ca.* 300 cm^{-1} (for λ and x about 170 cm^{-1} and 0.75, respectively), it is clear that the upper levels cannot be neglected in calculating susceptibilities at higher temperatures and not only because of their thermal population, since they also give rise to a large second-order Zeeman effect. So the corresponding Hamiltonian (9) may be written. The Hamiltonian matrix has

$$\hat{H} = -J\hat{S}_A\cdot\hat{S}_B - \beta H_z[2(\hat{S}_{A,z} + \hat{S}_{B,z}) - \tfrac{3}{2}x(\hat{L}_{A,z} + \hat{L}_{B,z})] \quad (9)$$

dimensions 144 × 144 [in general $12^m \times 12^m$, m being the number of cobalt(II) centres involved] and consequently the exact diagonalization becomes extremely difficult. In order to solve this problem and to obtain an analytical expression for the magnetic susceptibility, Lines used an approximate procedure: exact diagonalization of equation (9) is carried out within the ground Kramer's doublet, all other single-ion levels being neglected. The neglected upper levels are included in an effective field approximation. Thus, a hybrid theory results in which the exchange coupling is treated exactly within the ground Kramer's doublet, the excited single-ion levels being included as a molecular field. Such a theory is expected to be fairly accurate over the whole temperature range. It has the effect of replacing g_0 in equation (5) by a temperature-dependent g factor $[g(T)]$, the molar susceptibility for a cobalt(II) dimer being given by equation (10). In order to generate a theoretical χ_M *versus* T

$$\chi_M = (2N\beta^2[g(T)]^2/kT)[3 + \exp(-25J/9kT)]^{-1} \quad (10)$$

curve through equation (10) one needs to evaluate $g(T)$. This requires solution of the equations listed in the Appendix.

As a first step, we treated the experimental susceptibilities at $T < 30$ K in the context of the effective spin $s = \frac{1}{2}$ formalism through equation (5), but the computed curve did not match well the theoretical one. The large anisotropy of Co^{II} is at the origin of this bad fit and when it was taken into account [equations (6)–(8)] a good agreement between experimental and computed data was obtained. The values of the parameters J, $g_{\|}$, $g_{\perp}$ and R obtained by least-squares minimization are -5.20 cm^{-1}, 8.20, 2.12 and 3.9 × 10^{-4} for complex **1**, -4.63 cm^{-1}, 8.83, 1.20 and 4.4 × 10^{-4} for **2**, and -6.20 cm^{-1}, 8.20, 1.50 and 1.9 × 10^{-4} for **3**, respectively; R is the agreement factor defined as $\Sigma[(\chi_M)_{obs} - (\chi_M)_{calc}]^2/\Sigma[(\chi_M)_{obs}]^2$. In principle, this approximation is fairly good and correct values of J can be expected.

Secondly, we attempted to fit the experimental susceptibilities over the entire temperature range (300–4.2 K) through the Lines approach [equation (10)] and the computed curves matched well the experimental data as shown in Fig. 3. The best-fit parameters are collected in Table 8.

The interpretation of the experimental results for these complexes does not lead to an unambiguous choice of the values for x and λ. While a one-to-one correlation between x and λ/λ_0 (λ_0 is the free-ion spin–orbit coupling parameter, ≈ -170 cm^{-1}) is not expected, some concomitant reduction of x with λ/λ_0 is possible. A better understanding of the possible correlations involving the parameters x, λ/λ_0 and J can be achieved by an inspection of Fig. 4 which illustrates the effect of each parameter on the curve χ_M ($\chi_M T$) against T. It can be seen that the value of x is very dependent on the absolute value of $\chi_M T$ [Fig. 4(*a*)]: a reduction in x causes a proportional decrease in the values of $\chi_M T$ over the whole temperature range. However, λ exerts a small influence on $\chi_M T$ at high temperatures (> 150 K), its influence either on $\chi_M T$ or χ_M increasing when the temperature is lowered [Fig. 4(*b*)]. A similar effect is exerted by J. Nevertheless, the occurrence of a maximum in the molar susceptibility curve is due to the existence of an antiferromagnetic interaction and its position depends exclusively on the value of J. Although λ can change the height of the maximum, its position remains practically unmodified. As shown in Fig. 4(*b*), $T_{max} = 16$ K for values of λ varying from -90 to -170 cm^{-1}, whereas in Fig. 4(*c*) T_{max} is at 13, 16 and 19 K for $-J = 5$, 6 and 7 cm^{-1}, respectively. Therefore, the value of x is determined by the susceptibility data in the high-temperature range, whereas that of J is fixed by the position of the susceptibility maximum. The role of λ consists basically of tuning the shape of the curve (*i.e.* enhancing or reducing the decrease in $\chi_M T$ upon cooling) especially in the temperature range 50–150 K for complexes **1**–**3**, whereas J and x are the dominant factors for $T < 50$ K and > 150 K, respectively. Consequently the variation of $\chi_M T$ in the range 50–150 K will determine the value of λ. In this respect, the shape of the thermal dependence of the susceptibility for weakly coupled cobalt(II) dimers ($-J \leqslant 1$ cm^{-1}) is practically determined by the value of λ over the whole temperature range, and a good determination of this parameter can be made in this case. However, a correct estimation of λ is very difficult when dealing with cobalt(II) dimers exhibiting a strong intradimer exchange coupling ($-J > 20$ cm^{-1}) because J is now the leading parameter. So, the variable-temperature magnetic behaviour of most of the six-co-ordinated cobalt(II) dimers which exhibit relatively strong intradimer antiferromagnetic interactions can be

Table 8 Relevant structural data and best-fit parameters of complexes **1–3** obtained by treating the magnetic data by the Lines model

Compound	h^a/Å	$d_{Co\text{-}Co}{}^b$/Å	J/cm^{-1}	$z'J'{}^c$/cm^{-1}	λ^d/cm^{-1}	x^e	10^4R
1	0.048(1)	5.761(1)	−5.4	−0.001	−114	0.90	3.1
2	0.012(1)	5.782(1)	−4.7	−0.015	−97.3	0.94	1.1
3	0.141(1)	5.942(2)	−6.2	−0.008	−107.5	0.74	1.6

[a] The height of the metal atom from the best equatorial plane. [b] Metal–metal separation through bridging bipym. [c] Intermolecular interaction parameter. [d] Spin–orbit coupling. [e] Orbital-reduction factor.

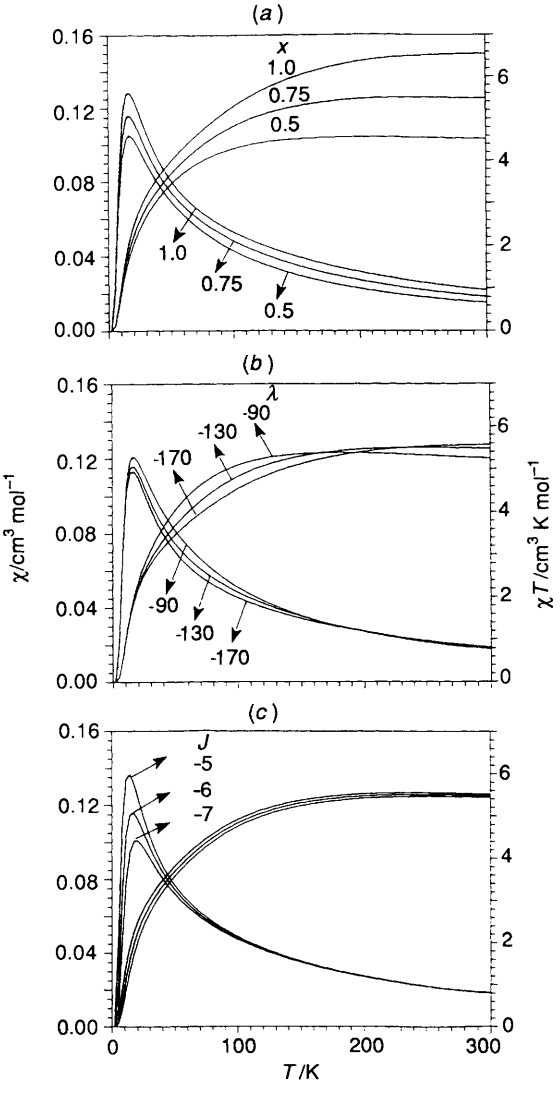

Fig. 4 Thermal dependence of $\chi_M T$ and χ_M for a cobalt(II) dimer as a function of x ($J = -6$ cm^{-1} and $\lambda = -130$ cm^{-1}) (*a*), λ ($J = -6$ cm^{-1} and $x = 0.75$) (*b*) and J ($\lambda = -130$ cm^{-1} and $x = 0.75$) (*c*)

described satisfactorily through the spin-only formalism [equation (1)], a value for the Landé factor g greater than 2 being allowed due to the possible orbital contribution. In the cases of intermediate magnetic coupling as for **1–3**, although a good agreement between experimental and calculated magnetic data can be obtained through the spin-only formula (especially when an important orbital reduction is operative), overestimates of J can be obtained because the effects of λ are included in J during the fit. If so, the temperature of the susceptibility maximum in the theoretical curve is greater than that of the experimental one.

From the above considerations it can be deduced that an accurate value of λ in the complexes **1–3** cannot be obtained because of the narrow range of temperature ($\Delta T < 100$ K) in which this parameter is dominant. In fact, variations of λ up to 20 cm^{-1} hardly worsen the quality of fit obtained with the parameters given in Table 8. This ambiguity does not allow one to differentiate the values of λ for complexes **1–3** ($\lambda \approx -100$ cm^{-1}). Moreover, these values of λ are too small, $\lambda/\lambda_0 \approx 0.6$. Although a reduction of λ can be expected due to covalency effects especially because of the presence of the ligand bipym (a strong-field ligand), such an important reduction seems unreasonable. The values of λ should be greater than that determined through Lines theory. This can be understood by taking into account that in the Lines approach octahedral symmetry is assumed for Co^{II} and the effects of a lowering of symmetry (partial breakdown of the degeneracy of the $^4T_{1g}$ state in the absence of spin–orbit coupling) on the magnetic properties are not considered. Figgis and co-workers[25] have investigated the magnetic properties of six-co-ordinated cobalt(II) complexes under the combined action of spin–orbit coupling and an axial ligand-field component. They showed that an increase in the value of the parameter v, defined as Δ/λ (Δ is the ^4A–^4E singlet–doublet energy gap), exerts a similar influence on the curve of μ_{eff} to that of a decrease in λ [Fig. 4(*b*)]. So, any splitting due to the ligand field would be translated into a decrease in the value of λ which is obtained by fitting the experimental magnetic data through the Lines theory. It is clear that such an extra decrease is a mathematical artifact and has no physical meaning for λ.

It is interesting that the orbital reduction in complex **3** ($x = 0.75$) is much greater than that of **1** and **2** ($x \approx 0.9$). Given that x would represent the t_{2g} electron delocalization, such a delocalization should be important in **3** and insignificant in **1** and **2**. The π-bonding pathway involved in the delocalization allows one to account for the different values of x: the co-ordinated water molecules present in **1** and **2** do not participate to a great extent in the π bonding, whereas the terminal thiocyanate and bipym ligands in **3** might well be expected to do so, and consequently to lead to an important reduction in the value of x.

The values of J for complexes **1–3** obtained through the Lines approach are practically identical to that obtained by the effective spin Hamiltonian formalism. This is expected because equations (6)–(8) are exact. The trend of the values of $-J$ closely follows the position of the susceptibility maximum: the higher T_{max}, the larger is the antiferromagnetic coupling. Even though the small differences observed in the values of $-J$ for **1–3** could be attributed to structural modifications (bond distances and angles around the metal ion), it is worthwhile noting that complex **3** being the most distorted and exhibiting the largest intramolecular metal–metal separation (see Table 8) shows the strongest antiferromagnetic coupling. This can be rationalized by considering the influence on J of the peripheral ligands, oxygen from water in **1** and **2** and N from thiocyanate in **3**. Extended-Hückel calculations in bipym-bridged metal complexes[26] have revealed that the less electronegative the peripheral atoms the greater is the exchange coupling. A comparison of the values of the exchange coupling in the series of structurally characterized bipym-bridged iron(II) dimers $[Fe_2(bipym)_3(NCS)_4]$ ($J = -4.1$ cm^{-1}),[12] $[Fe(H_2O)_8(bipym)][SO_4]_2{\cdot}2H_2O$ ($J = -3.4$ cm^{-1}) and $[Fe_2(H_2O)_6(bipym)(SO_4)_2]$ ($J = -3.1$ cm^{-1})[13] also illustrates this phenomenon.

Values of $-J$ ranging from 7 to 7.5 cm^{-1} were reported previously for a family of bipym-bridged cobalt(II) dimers of formula $[L_2Co(bipym)CoL_2]$ where the metal ion is surrounded by two nitrogens from bipym and four oxygens from the two acetylacetonato derivatives L.[10] In the light of the above considerations, these values should be closer to those of **1** and **2** (about 5 cm^{-1}). The origin of the discrepancy lies in the fact that the spin-only expression (1) was used to fit the experimental data. Furthermore, the fit was carried out on the $\chi_M T$ data and not on χ_M. The calculated χ_M curves do not match well the experimental ones in the vicinity of the maximum, the position of the theoretical maximum being shifted toward higher temperatures with respect to that of the observed one. Consequently, the values of the antiferromagnetic coupling in this series are overestimated and significantly reduced couplings would be obtained by considering the influence of λ.

The $z'J'$ term in Table 8, where z' is the number of neighbours and J' the exchange interaction parameter, accounts for the occurrence of interdimer interactions. Its values and their influence on the shape of the computed curve are so small that they can be neglected.

It is clear that the study of the exchange coupling between orbitally degenerate magnetic centres is a very difficult task. This is why the analysis of the magnetic behaviour of polynuclear complexes of Co^{II} was carried out through the simpler spin-only formalism. It should be noted that the analysis of the magnetic data at low temperatures, where only the ground Kramer's doublet is populated [equations (6)–(8)] provides correct J values. However, when the whole range of temperature (4.2–300 K) is considered the treatment of the magnetic data through equation (1) would lead to overestimates of J, except when strong antiferromagnetic coupling or important orbital reduction occurs. We think that although the Lines approach does not take into account deviations from the octahedral symmetry of Co^{II}, it is an essential tool to analyse the susceptibility data over the entire range of temperature.

Finally, the structures of the cobalt(II) dimers **1** and **2** as well as of analogous complexes of other divalent metal ions such as nickel(II), iron(II) and zinc(II) show that it is possible to obtain bipym-bridged dinuclear systems with terminal aqua ligands starting from simple stoichiometric metal : bipym molar ratios. These compounds are suitable examples to be used as models to investigate the influence of the nature of the peripheral ligands on the magnitude of the exchange coupling and also as building blocks to prepare large polymeric complexes by replacing the water molecules by other bridging ligands.

Appendix

Lines Equations for an Octahedral Cobalt(II) Dimer Exhibiting Isotropic Magnetic Exchange.—$\langle \hat{S}_z \rangle$ is the average molecular field from the excited levels, $= f(T)\hat{s}_z$, where $\hat{s}_z$ is a fictitious spin $\frac{1}{2}$ and H_0 is the applied field. The remaining parameters have the meanings indicated in the text. First, equations (A1)–(A11) are solved simultaneously for $\langle \hat{S}_z \rangle / \beta H_0$. This allows the values of parameters A and B to be determined, and with them $[g(T)]^2$ is calculated through equations (A12)–(A16). Secondly the value of χ_M (per dimer) is calculated through equation (10) in the text. The convergence in the process of simultaneous solution of equations (A1)–(A11) was attained when $|X_{i-1} - X_i| < 10^{-9}$ where $X_j = (\langle \hat{S}_z \rangle / \beta H_0)_j$.

$$f(T)\cdot g(T) = F/P \quad \text{(A1)}$$

$$F = F_1 + F_2E_1 + F_3E_2 \quad \text{(A2)}$$

$$P = 1 + 2E_1 + 3E_2 \quad \text{(A3)}$$

$$F_1 = (5/9)(10 + 3x - 15B) - (80/81)(kT/x\lambda)(4 + 3x - 6A) \quad \text{(A4)}$$

$$F_2 = (44/90)(22 - 6x - 33A) + (704/2025)(kT/x\lambda)(4 + 3x - 6A) \quad \text{(A5)}$$

$$F_3 = (21/5)(6 - 3x - 9A) + (16/25)(kT/x\lambda)(4 + 3x - 6A) \quad \text{(A6)}$$

$$E_1 = \exp(9x\lambda/4kT) \quad \text{(A7)}$$

$$E_2 = \exp(6x\lambda/kT) \quad \text{(A8)}$$

$$A = (1/3)(J + 2z'J')(\langle \hat{S}_z \rangle / \beta H_0) \quad \text{(A9)}$$

$$B = (1/3)(2z'J')(\langle \hat{S}_z \rangle / \beta H_0) \quad \text{(A10)}$$

$$(\langle \hat{S}_z \rangle / \beta H_0) = [f(T)g(T)/kT][3 + \exp(-25J/9kT)]^{-1} \quad \text{(A11)}$$

$$[g(T)]^2 = G/P \quad \text{(A12)}$$

$$G = G_1 + G_2E_1 + G_3E_2 \quad \text{(A13)}$$

$$G_1 = (1/9)(10 + 3x)(10 + 3x - 15B) - (40/81)(kT/x\lambda)(4 + 3x)(4 + 3x - 6A) \quad \text{(A14)}$$

$$G_2 = (2/45)(22 - 6x)(22 - 6x - 33A) + (352/2025)(kT/x\lambda)(4 + 3x)(4 + 3x - 6A) \quad \text{(A15)}$$

$$G_3 = (21/5)(6 - 3x - 9A) \times (16/25)(kT/x\lambda)(4 + 3x - 6A) \quad \text{(A16)}$$

Acknowledgements

Financial support from the Dirección General de Investigación Científica y Técnica (DGICYT) (Spain) through Project PB91-0807-C02-01 and from the Italian Ministero dell'Università e della Ricerca Scientifica e Tecnologica is gratefully acknowledged. Thanks are also due to A. Derory for magnetic measurements of compound **3** and to Servicio de Espectroscopía de la Universitat de València for instrumental facilities. We also thank the referees whose comments led to the inclusion of Fig. 4.

References

1 Part 3, G. De Munno and M. Julve, *Acta Crystallogr., Sect. C*, in the press.
2 (*a*) G De Munno and G. Bruno, *Acta Crystallogr., Sect. C*, 1984, **40**, 2030; (*b*) M. Julve, G. De Munno, G. Bruno and M. Verdaguer, *Inorg. Chem.*, 1988, **27**, 3160.
3 G. De Munno, G. Bruno, M. Julve and M. Romeo, *Acta Crystallogr., Sect. C*, 1990, **46**, 1828.
4 I. Castro, M. Julve, G. De Munno, G. Bruno, J. A. Real, F. Lloret and J. Faus, *J. Chem. Soc., Dalton Trans.*, 1992, 1739.
5 (*a*) M. Julve, M. Verdaguer, G. De Munno, J. A. Real and G. Bruno, *Inorg. Chem.*, 1993, **32**, 795; (*b*) G. De Munno, G. Bruno, F. Nicoló, M. Julve and J. A. Real, *Acta Crystallogr., Sect. C*, 1993, **49**, 457.
6 (*a*) G. De Munno, M. Julve, M. Verdaguer and G. Bruno, *Inorg. Chem.*, 1993, **32**, 2215; (*b*) L. W. Morgan, K. V. Goodwin, W. T. Pennington and J. D. Petersen, *Inorg. Chem.*, 1992, **31**, 1103; (*c*) L. W. Morgan, W. T. Pennington, J. D. Petersen and R. R. Ruminski, *Acta Crystallogr., Sect. C*, 1992, **48**, 163.
7 G. De Munno, M. Julve, F. Nicoló, F. Lloret, J. Faus, R. Ruiz and E. Sinn, *Angew. Chem., Int. Ed. Engl.*, 1993, **32**, 613.
8 G. De Munno, M. Julve, F. Lloret, J. Faus, M. Verdaguer and A. Caneschi, *Angew. Chem., Int. Ed. Engl.*, 1993, **32**, 1046.
9 G. De Munno, J. A. Real, M. Julve and M. C. Muñoz, *Inorg. Chim. Acta*, 1993, **211**, 227.
10 G. Brewer and E. Sinn, *Inorg. Chem.*, 1985, **24**, 4580.
11 G. De Munno, M. Julve, F. Lloret and A. Derory, *J. Chem. Soc., Dalton Trans.*, 1993, 1179.
12 J. A. Real, J. Zarembowitch, O. Kahn and X. Solans, *Inorg. Chem.*, 1987, **26**, 2939.
13 E. Andrés, G. De Munno, M. Julve, J. A. Real and F. Lloret, *J. Chem. Soc., Dalton Trans.*, 1993, 2169.

14 P. O. Kinell and B. Strandberg, *Acta Chem. Scand.*, 1959, **13**, 1607.
15 R. A. Bailey, S. L. Kozak, T. W. Michelson and W. N. Mills, *Coord. Chem. Rev.*, 1971, **6**, 407.
16 A. Earnshaw, *Introduction to Magnetochemistry*, Academic Press, London and New York, 1968.
17 A. C. T. North, D. C. Phillips and F. S. Mathews, *Acta Crystallogr., Sect. A*, 1968, **24**, 351.
18 SHELXTL PLUS, Version 3.4, Siemens Analytical X-ray Instruments Inc., Madison, WI, 1990.
19 M. Nardelli, *Comput. Chem.*, 1983, **7**, 95.
20 L. Fernholt, C. Rømming and S. Samdal, *Acta Chem. Scand., Ser. A*, 1981, **35**, 707.
21 P. M. Levy, *Phys. Rev. Lett.*, 1968, **20**, 1366; W. P. Wolf, *J. Phys. (Paris)*, 1971, **32**, C1-26.
22 R. J. Birgeneau, M. T. Hutchings, J. M. Baker and J. D. Riley, *J. Appl. Phys.*, 1969, **40**, 1070.
23 M. E. Lines, *J. Chem. Phys.*, 1971, **55**, 2977.
24 E. Coronado, M. Drillon, P. R. Nugteren, L. J. de Jongh and D. Beltrán, *J. Am. Chem. Soc.*, 1988, **110**, 3907.
25 B. N. Figgis, M. Gerloch, J. Lewis, F. E. Mabbs and G. A. Webb, *J. Chem. Soc. A*, 1968, 2086; M. Gerloch and P. N. Quested, *J. Chem. Soc. A*, 1971, 3729.
26 F. Lloret, M. Julve, J. Cano and S. Alvarez, unpublished work.

Received 13*th October* 1993; *Paper* 3/06121C